Προσομοίωση Καμπτικών Μορφών Αστοχίας Μελών ΟΣ Υποβαλλόμενων σε Ισχυρές Σεισμικές Φορτίσεις

Modeling RC Members Flexural Failure Modes under Severe Seismic Loading

Ilias A. Gkimousis[1], Vlasis K. Koumousis[2]

Λέξεις κλειδιά: Ανελαστικό προσομοίωμα σκυροδέματος, Ανακυκλιζόμενη συμπεριφορά ράβδου οπλισμού, Λυγισμός ράβδου οπλισμού, Μη-γραμμική ανάλυση

Keywords: Plastic-Damage Concrete Model, Rebar Steel Cyclic Behavior, Rebar Buckling, RC Column Failure, RC Nonlinear Analysis

ΠΕΡΙΛΗΨΗ: Ο στόχος της παρούσας εργασίας επικεντρώνεται στην αριθμητική προσομοίωση των καμπτικών μορφών αστοχίας μελών ΟΣ, αναδεικνύοντας έτσι την ακριβή απόκριση πλαισίων σε ισχυρές σεισμικές διεγέρσεις κοντά στην κατάρρευση τους. Για το σκοπό αυτό αναπτύσσεται ένα μονοαξονικό προσομοίωμα χάλυβα οπλισμού που ενσωματώνει τη μη-γραμμική κινηματική και ισοτροπική κράτυνση, περιγράφοντας επίσης το φαινόμενο του ανελαστικού λυγισμού. Παράλληλα, αναπτύσσεται το μονοαξονικό προσομοίωμα σκυροδέματος που συνδυάζει τη θεωρία πλαστικότητας και μηχανικής των βλαβών, έτσι ώστε να περιγράφει τα φαινόμενα της σύνθλιψης πυρήνα και της αποφλοίωσης της επικάλυψης. Η αποφλοίωση έχει το επιπλέον χαρακτηριστικό της ενεργοποίησης του μηχανισμού λυγισμού των ράβδων. Τα προτεινόμενα προσομοιώματα ενσωματώνονται σε ένα πεπερασμένο στοιχείο δοκού-υποστυλώματος, η αποδοτικότητα και ακρίβεια του οποίου τεκμηριώνεται με σύγκριση με σεισμικά πειραματικά αποτελέσματα σε ένα τριώροφο πλαίσιο από ΟΣ.

ABSTRACT: The aim of this work is to model flexural failure modes of RC members revealing reliably the overall response of RC structures under intensive seismic loading near collapse. More specifically, rebar inelastic behavior is addressed by developing a uniaxial stress-strain constitutive relation which is based

[1] Δρ Πολιτικός Μηχανικός, Σχολή Πολιτικών Μηχανικών, Εθνικό Μετσόβιο Πολυτεχνείο, email: cvgkim@central.ntua.gr

[2] Καθηγητής, Σχολή Πολιτικών Μηχανικών, Εθνικό Μετσόβιο Πολυτεχνείο, email: vkoum@central.ntua.gr

on a combined nonlinear kinematic and isotropic hardening law, while also inelastic buckling in compression is addressed. In addition, a smooth plasticity-damage model is developed for concrete, accounting for uniaxial compressive-tensile behavior and nonlinear unloading. This is used to address concrete core crushing and spalling, which eventually triggers the inelastic buckling of longitudinal rebars. The proposed models for concrete and rebars are embedded into a properly adjusted fiber beam-column element and the proposed formulation is verified with existing experimental data on a RC plane frame under extreme seismic loading.

INTRODUCTION

Typical flexural failure modes of RC columns undergoing intensive cyclic loading are usually attributed to significant spalling, concrete crushing and rebar buckling. When reinforcing bars deform under high compressive strains at intensive cyclic loading, they may induce buckling in the form of large lateral deformations between either adjacent stirrups, or a wider area including one or more drifted stirrups.

To model nonlinear response from linear elastic behavior until collapse, the distributed plasticity concept using fiber discretization technic is used (Spacone et al., 1996). This allows treatment of the RC beam-column element in the control sections using uniaxial constitutive laws, hence, rendering this procedure computationally attractive. Along the lines of fiber modeling, a uniaxial rate coupled plastic-damage concrete model able to simulate core crushing and cover spalling that triggers rebar buckling mechanism is developed. The concrete model can describe softening and stiffness degradation behavior, while it is also enriched with nonlinear unloading. Alongside, considering uniaxial rebar models including inelastic buckling, a model that describe local rebar buckling is proposed where reinforcing bars buckle following the local buckling mode between two adjacent stirrups. Following the works of Massone and Moroder (2009) and Urmson and Mander (2012), steel rebar is simulated as a beam element where average strains are the problem's input and average stresses are the problem's output. Buckling curve and curvature distribution are derived analytically as soon as concrete cover spalls and the numerical procedure results in an incremental scheme where mid-length curvature is updated until equilibrium at the deformed state is attained. The point wise cyclic steel model developed combines nonlinear kinematic and isotropic hardening with yield plateau, rendering the proposed rebar model capable of expressing various types of cyclic response. Finally, the concrete and rebar models are embedded into a global variationally consistent mixed fiber model (Gkimousis and Koumousis, 2016), while its accuracy is tested against experimental data.

REBAR CONSTITUTIVE MODEL

Cyclic steel uniaxial model

The cyclic steel model is developed following the fundamentals of classical plasticity and the respective stress-strain law is expressed in rate form as:

$$\dot{\sigma} = \left[1-(1-\alpha)\cdot H_1 \cdot H_2\right]\cdot E\cdot\dot{\varepsilon} \;=\; E_t\cdot\dot{\varepsilon} \tag{1}$$

where, α is the post to pre-yield stiffness ratio.

Equation (1) describes steel uniaxial cyclic behavior in the full nonlinear path ranging from linear elastic loading to plastic flow and elastic unloading. This is accomplished by the two Heaviside functions H_1 and H_2 acting as "switches". More specifically, function H_1 controls yielding (0: elastic phase, 1: plastic phase) while H_2 controls loading/unloading (0: unloading state, 1: loading state). Consequently, H_1 emerges from the smoothening of the yield function and the following relation holds:

$$H_1 = \left|\frac{\sigma-b}{r}\right|^n \tag{2}$$

where, n controls the transition smoothness from the elastic to plastic branch of the stress-strain law. In addition, function H_2 aims at controlling loading and unloading following the sign of the yield function rate with positive sign indicating loading while negative sign unloading:

$$H_2 = 0.5\cdot\left[1+sgn\left((\sigma-b)\cdot\dot{\varepsilon}\right)\right] \tag{3}$$

In relations (2) and (3) b is the back stress describing nonlinear hardening, which is implemented in the proposed model following the Armstrong-Frederick evolution equation:

$$\dot{b} = \;(1-m)\cdot H\cdot\dot{\lambda}\cdot sgn(\sigma-b) \tag{4}$$

where, m is the percentage of isotropic hardening to the model. A further modification is applied in function H_2 that corrects incompatibility with Drucker's

or Ilyushin's postulates of plasticity for partial unloading-reloading, i.e. short reversals in the nonlinear path. Hence, function H_2 obtains the following form:

$$\overline{H}_2 = H_2 \cdot (1 - R) \tag{5}$$

where, R is a stiffening factor that controls stiffness recovery in the reloading branch and the appropriate formula is developed in Charalampakis and Koumousis (2009). Finally, the proposed steel model with all the additional features is illustrated in Figure 1

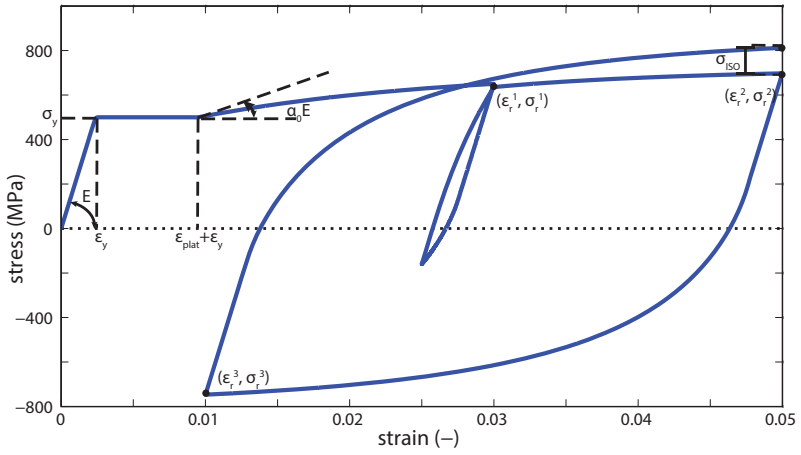

Figure 1. Presentation of the proposed uniaxial steel model

Rebar buckling model

Local buckling is addressed under the assumption that transverse ties are practically rigid, hence a single longitudinal bar is modeled as fixed end beam with an axial force (Figure 2). According to Euler elastic buckling theory, a rebar deflects laterally following a cosine curve:

$$y(x) = \frac{e}{2} \cdot \left(1 - \cos\left(\frac{2\pi x}{L} \right) \right) \tag{6}$$

Rotation $\theta(x)$ along bar's length is derived by differentiating the displacement field as:

$$\theta(x) = \frac{e\pi}{L} \cdot \sin\left(\frac{2\pi x}{L}\right) \tag{7}$$

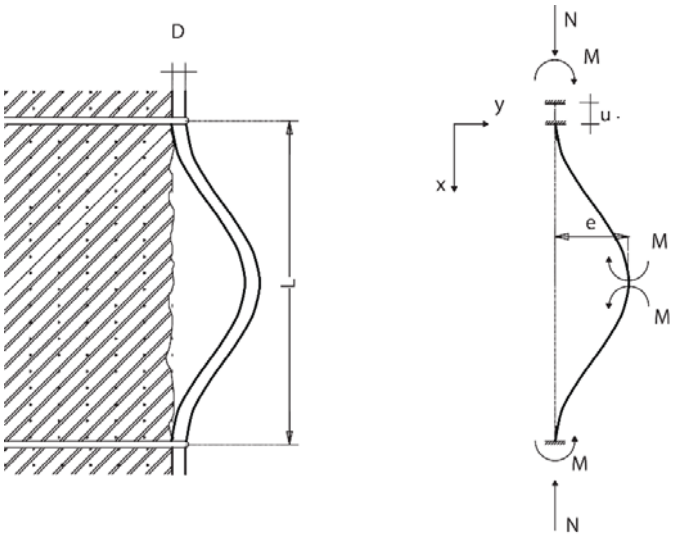

Figure 2. Local buckling physical and computational model

The axial shortening of the rebar is expressed in terms of the axial force and rotation according to the following relation:

$$u = u(L) - u(0) = \int_0^L \left(1 - \cos\theta + \frac{P}{EA}\cos^2\theta\right) dx \tag{8}$$

Expressing *cosθ* function in Taylor series and performing the integration using relation (7), axial shortening obtains the form:

$$u = \frac{PL}{EA} + \frac{\left(1 - \frac{2P}{EA}\right)\pi^2 e^2}{4L} - \frac{\left(1 - \frac{8P}{EA}\right)\pi^4 e^4}{64L^3} \tag{9}$$

Consequently, the average axial strain that is imposed at the rebar fiber during the state determination process is simply expressed as:

$$\varepsilon_{av} = \frac{u}{L} = \frac{P}{EA} + \frac{\left(1 - \frac{2P}{EA}\right)\pi^2 e^2}{4L^2} - \frac{\left(1 - \frac{8P}{EA}\right)\pi^4 e^4}{64L^4} \tag{10}$$

Moreover, total average axial strain ε_{av} over the length of the bar can be decomposed into the sum of the 1st order strain ε_0 at the centroid of the rebar cross section and the buckling strain ε_b caused by the additional shortening due to the lateral deflection and the resulting curvature field.

$$\varepsilon_{av} = \varepsilon_0 + \varepsilon_b \tag{11}$$

As a result the buckling strain ε_b results from relation (10) for the axially inextensible case $(EA \to \infty)$ eliminating also higher order effects:

$$\varepsilon_b = \frac{\pi^2 e^2}{4L^2} \tag{12}$$

Finally, the tangent material modulus of the rebar fiber, necessary for the quadratic convergence of the global iterative scheme, is derived from equation (9), solving for the axial force P and then calculating the derivative:

$$E_{\tan} = \frac{d\sigma_{av}}{d\varepsilon_{av}} = \frac{dP}{du} \cdot \frac{L}{A} = \frac{2EI^2}{2L^2 - \pi^2 e^2} \tag{13}$$

CONCRETE CONSTITUTIVE MODEL

Concrete under low stress level exhibits linear elastic behavior but soon after the first cracks appear a nonlinear behavior with irreversible features both in strain and stiffness terms is established. Friction along crack edges prevents the cracks from prolonged opening without resistance. This process is manifested macroscopically as elastoplastic behavior with a nonlinear isotropic hardening branch. Consequently, stress-strain constitutive relation due to plasticity is expressed as follows:

$$\dot{\bar{\sigma}}_c = \left(1 - (1 - \alpha_c) \cdot H_{c1} \cdot H_{c2}\right) \cdot E_c \cdot \dot{\varepsilon}_c \tag{14}$$

where $\bar{\sigma}_C$, ε_C are concrete's uniaxial effective stress and strain, $\alpha_{C,i}$ defines post-yield to pre-yield stiffness ratio and H_{C1}, H_{C2} are Heaviside type functions acting as switches.

Soon after initial loading, cracks are formed and the effective reference volume at the critical region of the RC member is reduced. By applying the strain equivalent damage theory (Kachanov, 1986) the true concrete stress is calculated from the effective undamaged stress using relation:

$$\sigma_c = (1-D)\cdot\bar{\sigma}_c \tag{15}$$

where D is the time dependent damage parameter which quantifies damage caused in tension and compression field according to the following relation:

$$D_i = 1 - e^{-\left(\frac{k_i - k_{0,i}}{b_i k_{0,i}}\right)^{P_i}} \tag{16}$$

It is evident from experiments that concrete exhibits nonlinear unloading, whereas in reloading it remains linear, altering in such way the hysteretic loops. This behavior is incorporated in a phenomenological manner into the model by introducing the unloading function $r_{un}(\bar{\sigma}_C, \bar{\sigma}_{C,r})$ that modifies the tangent concrete modulus $E_{C,t}$:

$$r_{un} = \left(c_1 \left| \frac{\bar{\sigma}_c}{\bar{\sigma}_{c,r}} \right| + c_2 \right)^{1-H_{c2}} \tag{17}$$

where exponent $1-H_{c2}$ activates/deactivates unloading function, c_1, c_2 are model parameters and $\bar{\sigma}_{c,r}$ is the effective stress at the reversal point. Finally, combining all previous effects the stress-strain constitutive relation of concrete can be written according to the following equation (18) (Andriotis et al., 2015):

$$\begin{aligned} \dot{\sigma}_c &= E_{c,t}\cdot\dot{\varepsilon}_c \\ E_{c,t} &= \left\{ (1-D)\cdot\left[1-(1-a)\cdot H_{c1}\cdot H_{c2}\right] - \left(H_{c4}\cdot H_{c2}\cdot\frac{dD_i}{dk_i}\cdot\frac{\bar{\sigma}_c}{E_i} \right) \right\} \end{aligned} \tag{18}$$

In Figure 3 the proposed concrete model is presented where all the aforementioned phenomena are illustrated.

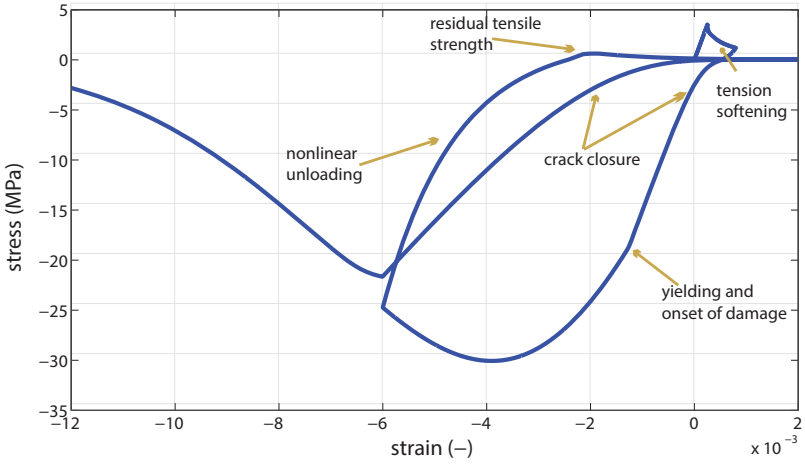

Figure 3. The proposed concrete model.

NUMERICAL EXAMPLE

Experimental setting description and input data

In this example the numerical model is tested against a 3-storey, 3-bay frame tested dynamically by Ghannoum and Moehle (2012) on the University of California, Berkeley shake table. The frame is a one-third scale planar specimen representing a typical strong beam, weak column design office building of the 1960s. Structure's geometry and reinforcing details are presented in **Figure 4**. More specifically, it consists of two different types of column detailing, as half left side columns (C1-C3, D1-D3) are designed according to modern design provisions (ACI 318-08) for moment resisting frames with high ductility. On the other hand, the right half side columns (A1-A3, B1-B3) are dimensioned to represent typical columns of the 1960s with widely spaced ties closed with 90 degrees hoops. The RC frame is dynamically tested with a record obtained during March 3, 1985, Chile earthquake which is presented in **Figure 5**. The original ground motion is amplified with a scale factor of *4.06* in order to enforce the frame RC structure to reach its ultimate strength capacity.

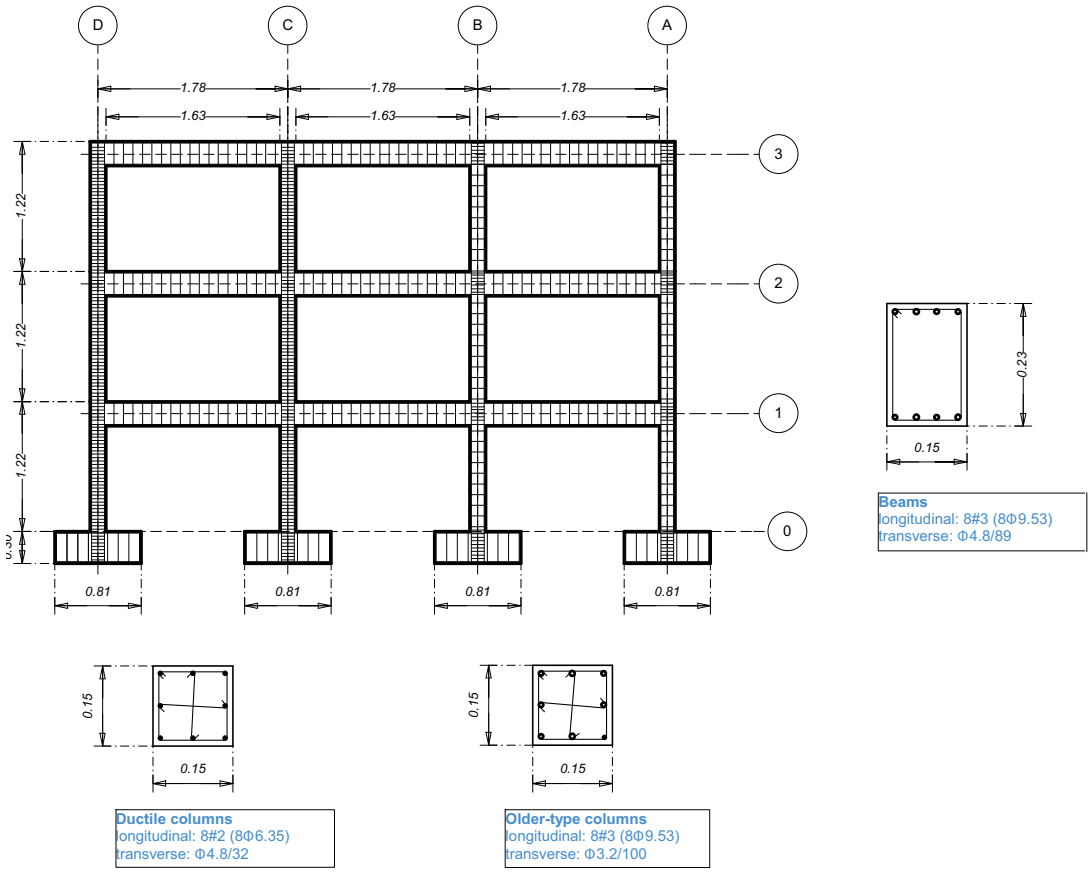

Figure 4. 3-storey, 3-bay frame dimensions and reinforcing details

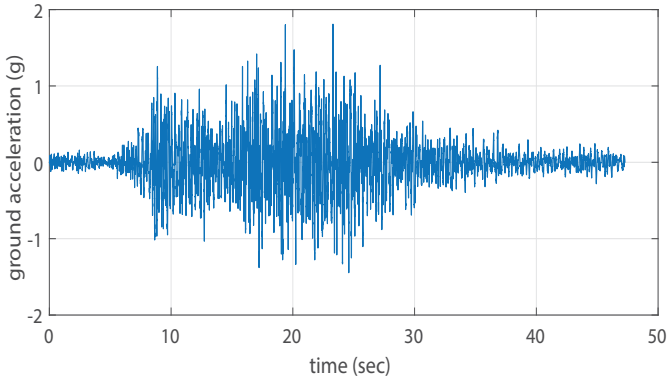

Figure 5. Ground motion input (Chile Valparaio 1985 Llolleo x 4.06)

Considering material properties, rebar yield stress is $\sigma_y=475\ MPa$, while steel rebar parameters are seletected to represent typical stress strain hysteretic loops. Concrete strength was measured to be $\sigma_c=24.6\ MPa$ at the day of the experiment, while secant modulus at the stress level of $0.4\sigma_c$ is $E_c=19\ MPa$. In the case of the confined concrete fibers, the Mander et al. (1988) model was used to calculate the maximum confined compressive strength. Confinement factor k obtains value $k=1.9$ for the confined columns ($\sigma_{cc}=k\cdot\sigma_c=46.7\ MPa$) and $k=1.1$ for the older-type columns ($\sigma_{cc}=k\cdot\sigma_c=27.2\ MPa$).

Every span of the frame is loaded with a uniformly distributed load of $16.67\ KN/m$, considering also its vertical mass contribution. The flexibility at the footings was included in the numerical model with rotational springs. Spring stiffness was selected in such way that the fundamental elastic eigenperiod of the numerical model to match the fundamental eigenperiod ($T_1=0.34\ sec$) of the frame specimen which was measured experimentally. Following this procedure, spring stiffness value is $K_{spring}=6500\ KNm/rad$.

Numerical analysis and comparison

A variationally consistent mixed fiber beam-column element developed by the authors (Gkimousis and Koumousis, 2016) is implemented in the analysis. Element discretization scheme consists of *4* Gauss-Lobatto integration points for the columns, resulting in a localization plastic-hinge zone of *83 mm* at both column ends. Fiber discretization consists of 12 layers for the sections cover and 30 layers for the section core.

Initially, comparison with experimental results performed in terms of frame interstorey drift and base shear. Indeed, in **Figure 6** and **Figure 7** 1st storey drift and base shear time histories for both numerical analysis and experiment are plotted for the time period between 10 sec and 35 sec where the significant nonlinear response is observed.

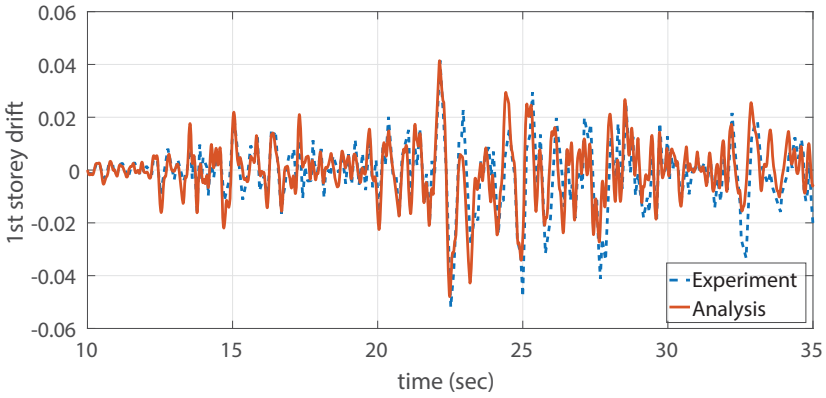

Figure 6. 1st storey drift comparison

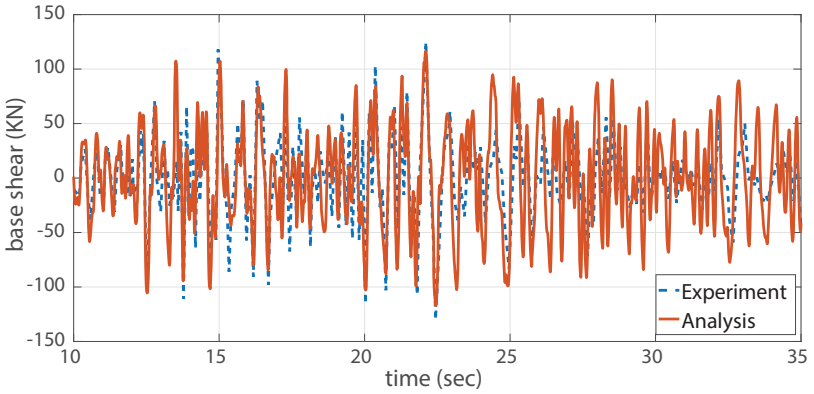

Figure 7. Base shear comparison

In **Figure 8** horizontal drift ratio versus shear force at the base of the older type column A1 is presented. Numerical modeling is able to capture quite accurately the initial stable cycles of shear response vs the drift range. It is interesting that column A1 presents reduced shear force in the negative direction. During reloading half-cycle, after column reaches shear force of nearly *40 KN* it experiences tensile axial loading which reduces its compression zone, diminishing on the same time its strength capacity.

In addition, comparison is performed in **Figure 8** for the same column in terms of deformations, where the range of chord rotations is almost perfectly predicted.

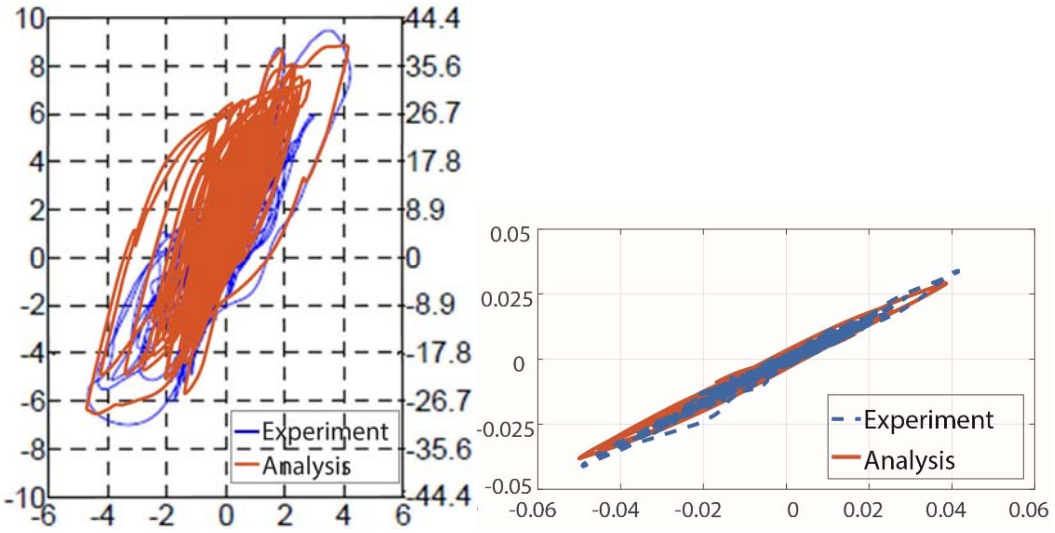

(a) (b)

Figure 8: (a) Horizontal drift vs base and (b) Horizontal drift vs chord rotations comparison for column A1 bottom end section

REFERENCES

Andriotis, C., Gkimousis, I., Koumousis, V. (2015). "Modeling Reinforced Concrete Structures Using Smooth Plasticity and Damage Models." J. Struct. Eng., Volume 142, Issue 2.

Charalampakis, A.E. & Koumousis, V.K., "A Bouc-Wen model compatible with plasticity postulates." Journal of Sound and Vibration, 322(4-5) (2009) 954-968.

Ghannoum, W.M. & Moehle, J.P., "Shake-Table Tests of a Concrete Frame Sustaining Column Axial Failures." ACI Structural Journal, 109(3) (2012) 393-402.

Gkimousis, I.A. & Koumousis, V.K., "Inelastic mixed fiber beam finite element for steel cyclic behavior." Engineering Structures, 106 (2016) 399-409.

Kachanov, L. «Introduction to Continuum Damage Mechanics» Martinus Nijhoff Publishers, Dordrecht, The Netherlands (1986).

Mander, J.B., Priestley, M.J.N. & Park R., "Theoretical stress-strain model for confined concrete." Journal of Structural Engineering, ASCE, Vol. 114, 8 (1988) 1804-1826.

Massone, L. & Moroder, D., “Buckling modeling of reinforcing bars with imperfections.” Eng Struct, 31(3) (2009) 758-67.

Spacone, E., Ciampi, V. & Filippou, F.C., “Mixed formulation of nonlinear beam element.” Computers and Structures, Vol. 58 No. 1 (1996a) 71-83.

Urmson, C.R. & Mander, J.B., “Local buckling analysis of longitudinal reinforcing bars.” Journal of Structural Engineering, 138 (1) (2012) 62-71.